

Supplement of Atmos. Meas. Tech., 7, 4417–4430, 2014
<http://www.atmos-meas-tech.net/7/4417/2014/>
doi:10.5194/amt-7-4417-2014-supplement
© Author(s) 2014. CC Attribution 3.0 License.



Supplement of

Online derivatization for hourly measurements of gas- and particle-phase semi-volatile oxygenated organic compounds by thermal desorption aerosol gas chromatography (SV-TAG)

G. Isaacman et al.

Correspondence to: G. Isaacman (gabriel.isaacman@berkeley.edu)

1 **S1. Derivatization efficiency tests**

2 As discussed in the text, derivatization efficiency is tested using repeated injection of a mixture
3 including 43 oxygenated compounds. In Table S1, names of the compounds injected and their
4 molecular formulas and number of OH groups are shown, as well as the retention index of the
5 derivatized compound. For every OH group, the derivatized compound eluted contains a
6 trimethylsilyl group, adding C_3H_8Si to the formula of the observed peak. Observed relative
7 retention times are shown as a Kovats-like (Kovats, 1958) retention index relative to *n*-alkanes,
8 with i.e. *n*-pentacosane (C_{15}) having an index of 1500. Compounds span a retention time of
9 approximately tridecane to tetratriacontane, but most (38 compounds) elute earlier than
10 pentacosane.

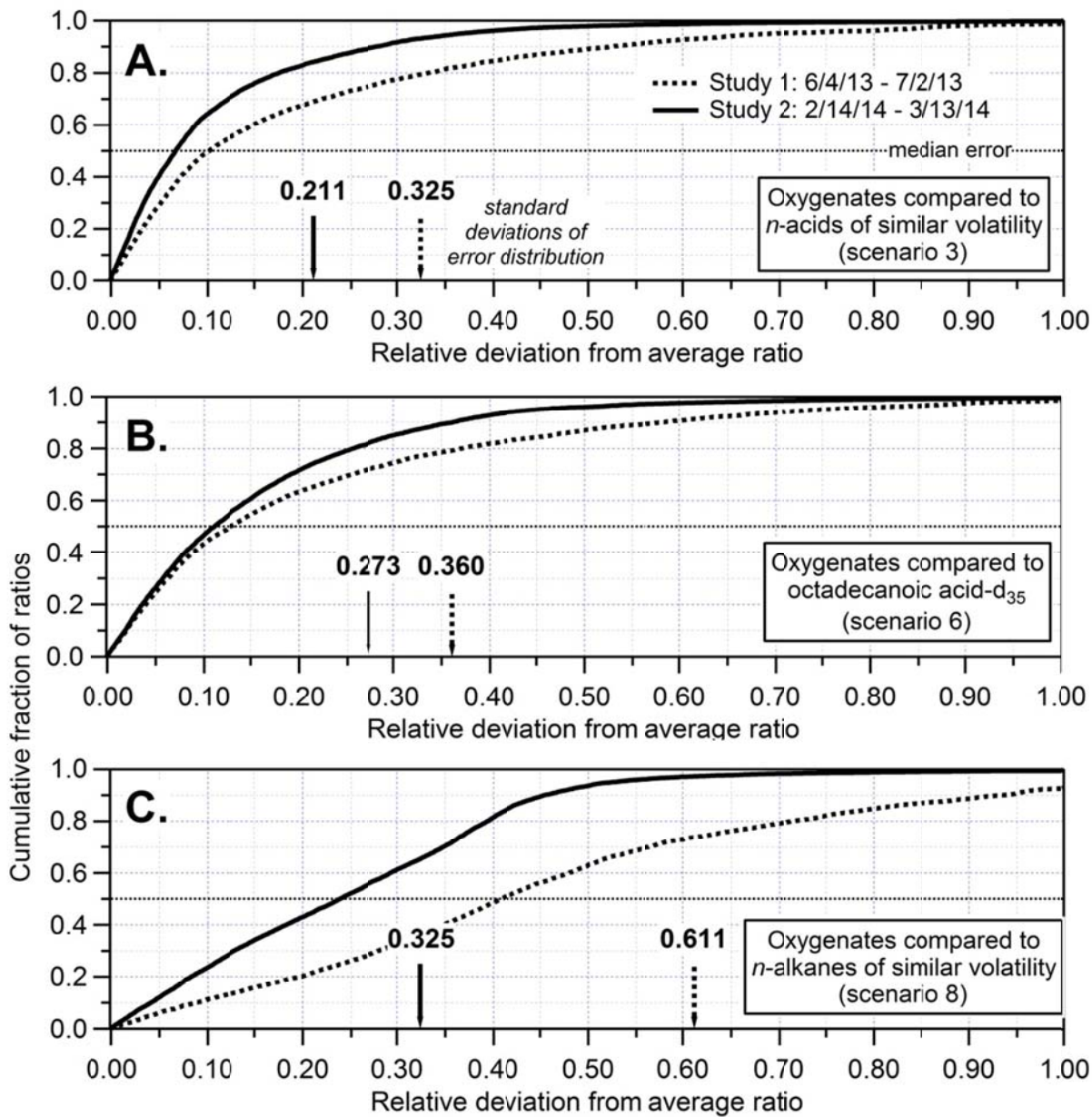
11

12 Table S1. Compounds injected to assess derivatization efficiency: name, molecular formula,
 13 number of OH groups, and retention index of the derivatized peak relative to an *n*-alkane series.

Injected Compound Name	Molecular Formula	Number OH Groups	Derivatized Retention Index
Glyceric acid	C ₃ H ₆ O ₄	3	1323
2,6-Dimethoxyphenol (Syringol)	C ₈ H ₁₀ O ₃	1	1398
3,3-Dimethylglutaric acid	C ₇ H ₁₂ O ₄	2	1433
<i>n</i> -Decanoic acid	C ₁₀ H ₂₀ O ₂	1	1453
Threitol	C ₄ H ₁₀ O ₄	4	1493
Erythritol	C ₄ H ₁₀ O ₄	4	1501
Ketopinic acid	C ₁₀ H ₁₄ O ₃	1	1507
<i>cis</i> -Pinonic acid	C ₁₀ H ₁₆ O ₃	1	1526
3-Methoxy-4-hydroxybenzaldehyde (Vanillin)	C ₈ H ₈ O ₃	1	1537
2-Methoxy-4-propenylphenol (Isoeugenol)	C ₈ H ₁₀ O ₃	1	1568
Diethyltoluamide	C ₁₂ H ₁₇ NO	0	1582
Benzophenone	C ₁₃ H ₁₀ O	0	1645
<i>cis</i> -Pinic acid	C ₉ H ₁₄ O ₄	2	1663
γ -Dodecalactone	C ₁₂ H ₂₂ O ₂	0	1688
Levogluconan	C ₆ H ₁₀ O ₅	3	1698
α -Bisabolol	C ₁₅ H ₂₆ O	1	1742
<i>n</i> -Tridecanoic acid	C ₁₃ H ₂₆ O ₂	1	1746
1,9-Nonadioic acid	C ₉ H ₁₆ O ₄	2	1791
1,10-Decadioic acid	C ₁₀ H ₁₈ O ₄	2	1887
Methyl palmitate	C ₁₇ H ₃₄ O ₂	0	1924
<i>n</i> -Hexadecanol	C ₁₆ H ₃₄ O	1	1956
<i>cis</i> -9-Hexadecenoic acid	C ₁₆ H ₃₀ O ₂	1	2022
Homosalate	C ₁₆ H ₂₂ O ₃	1	2025
<i>n</i> -Hexadecanoic acid	C ₁₆ H ₃₂ O ₂	1	2041
1,12-Dodecadioic acid	C ₁₂ H ₂₂ O ₄	2	2082
Methyl stearate	C ₁₉ H ₃₈ O ₂	0	2125
<i>n</i> -Heptanoic acid	C ₁₇ H ₃₄ O ₂	1	2139
<i>n</i> -Octadecanol	C ₁₈ H ₃₈ O	1	2154
<i>cis,cis</i> -9,12-Octadecadienoic acid	C ₁₈ H ₃₂ O ₂	1	2206
<i>cis</i> -9-Octadecenoic acid	C ₁₈ H ₃₄ O ₂	1	2213
<i>cis</i> -11-Octadecenoic acid	C ₁₈ H ₃₄ O ₂	1	2220
<i>n</i> -Octadecanoic acid	C ₁₈ H ₃₆ O ₂	1	2240
1,14-Tetradecanoic acid	C ₁₄ H ₂₆ O ₄	2	2275
<i>n</i> -Eicosanol	C ₂₀ H ₄₂ O	1	2349
Isopimaric acid	C ₂₀ H ₃₀ O ₂	1	2353
16-Hydroxyhexadecanoic acid	C ₁₆ H ₃₂ O ₃	2	2385
12-Hydroxyoctadecanoic acid	C ₁₈ H ₃₆ O ₃	2	2423
Abietic acid	C ₂₀ H ₃₀ O ₂	1	2433
Deoxycholic Acid	C ₂₄ H ₄₀ O ₄	3	3065
Cholesterol	C ₂₇ H ₄₆ O	1	3166
β -Stigmasterol	C ₂₉ H ₄₈ O	1	3297
β -Sitosterol	C ₂₉ H ₅₀ O	1	3360
Lupeol	C ₃₀ H ₅₀ O	1	3441

14 **S2. Derivatization reproducibility tests**

15 When correcting analytes for run-to-run variability using internal standards, an internal standard
16 must be selected to use for the correction. Several possible selection criteria are available for
17 correction of oxygenated compounds. Table 1 in the main text lists the schemes tested for
18 correction of all oxygenates with hydroxyl groups and the error of each scenario, measured as the
19 relative standard deviation from the average ratio of one internal standard to another one selected
20 based on the criteria of the scenario. Figure S1 shows the cumulative error distribution for a
21 subset of the test scenarios selected to apply to most, if not all, operating conditions. Correcting
22 for compounds using an internal oxygenated standard of only similar volatility (i.e. in the case of
23 analytes of unknown structure or a functionally similar internal standard is unavailable) is
24 modeled by correcting all oxygenates to the nearest *n*-acid in volatility, of which there are 4 of
25 various volatility in the standard used (Fig. S1a). The error present in correcting for only general
26 changes in derivatization efficiency is quantified by correcting all oxygenates using a single,
27 relatively stable oxygenate, *n*-octadecanoic acid- d_{35} (Fig. S1b). Under operating conditions
28 requiring minimal internal standards or maximizing standard stability by not including
29 oxygenates, oxygenates can be corrected for variability in transfer efficiency and detector
30 sensitivity using only alkanes of similar volatility, but this results in large errors with a relatively
31 non-Gaussian distribution (Fig. S1c). Due in part to operational improvements after the SOAS
32 field campaign, Study 2 has lower error in all cases shown in Fig. S1 owing to more reproducible
33 measurements of multi-functional acids.



34
 35 Figure S1. Cumulative distribution of error in correction of oxygenates for run-to-run variability
 36 in derivatization efficiency and instrument response measured as relative deviation of two
 37 internal standards from their average ratio. Boxes and Sect. S2 describe each correction scenario,
 38 which are numbered corresponding to Table 1 in the main text. Arrows show relative standard
 39 deviation for each study. Dotted line is median error (50% of points halve less than this error).

40

41 **S3. Total uncertainty**

42 The main text of this manuscript addresses reproducibility and precision in derivatization. To
43 explicitly calculate total uncertainties in reported masses and fractions in the particle, the two
44 independent cells of the instrument also have to be calibrated and then compared. Uncertainty in
45 mass calibration using a linear calibration curve is described by NIST (2014a) and is applied in
46 Sect. S3.1 without significant modifications to recommended practices. Differences between
47 parallel sampling cells are removed through normalization to the mean response of the two cells
48 to identical samples, with the magnitude and uncertainty in this normalization included in
49 estimation of mass uncertainty as described in Sect. S3.2. Finally, in Sect. S3.3, uncertainty in
50 particle fraction is found to be a function of this normalization, as well as derivatization precision
51 as discussed in the main text, but not mass calibration.

52 Known compounds are found below to be quantified with 20-25% accuracy, though detailed
53 error analysis is actually compound-, study-, and even point-specific. By calculating fraction in
54 particle before performing mass calibration, partitioning can be measured with less uncertainty
55 than simply compounding the error in two compared mass measurements. Fraction in particle is
56 thus found to also be measured with approximately 15-25% uncertainty; formal estimation of
57 this error is confirmed through empirical estimates. Calculating F_P from signals also allows
58 measurement of particle fraction even for compounds which are not unambiguously identified or
59 for which no authentic standard exists. Data from this instrumented is found to be best reported
60 as total mass and fraction in the particle, with particle mass calculated from these two value,
61 because particle mass is typically lower and thus more uncertain than total mass.

62

63 **S3.1. Uncertainty in mass calibration of a single cell**

64 Raw signal, R_A^i , of an analyte in either cell, i , is ratioed to the raw signal of an internal standard,
65 R_{IS}^i , to generate a corrected signal, S_A^i , that accounts for any systematic variability in instrument
66 response. The uncertainty in this correction for run-to-run variability is detailed in the main text
67 and is defined here as σ_S^i , a relative uncertainty in precision. It depends on the similarity between
68 the analyte and the internal standard, but in typical operation is usually 10-15% depending on the
69 compound (and includes uncertainty in the AutoInject injections).

70 Calibration curves as shown in Fig. 5 are calculated in terms of calibrant corrected signal, S_C^i ,
 71 (raw calibrant signal, R_C^i , ratioed by internal standard, R_{IS}^i), against mass injected (using the
 72 AutoInject) for all injections within a given operational period. A linear fit of calibrants ($S_C^i =$
 73 $a^i + b^i M_C^i$) is used, such that the mass of an analyte M_A^i is:

$$74 \quad M_A^i = \frac{S_A^i - a^i}{b^i} \quad (\text{Eq. S1})$$

75 Absolute error in mass for any point, j , $\Delta_{M_j}^i$, is derived from the linear fit (NIST, 2014a):

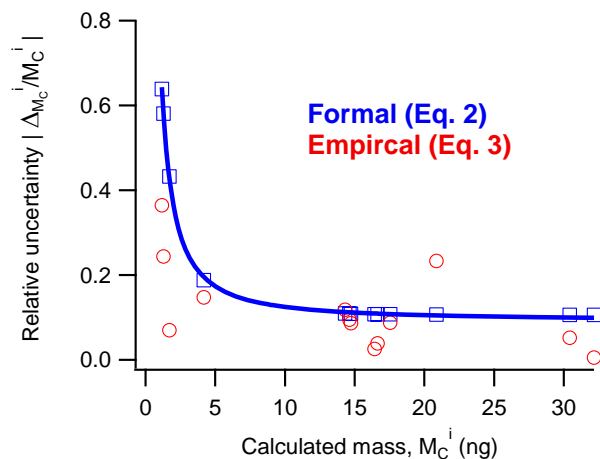
$$76 \quad \Delta_{M_j}^i = \sqrt{\left(\frac{1}{b^i}\right)^2 \Delta_S^i{}^2 + \left(\frac{-1}{b^i}\right)^2 \Delta_a^i{}^2 + \left(\frac{-(S_{A_j}^i - a^i)}{b^i{}^2}\right)^2 \Delta_b^i{}^2 + 2 \left(\frac{-1}{b^i}\right) \left(\frac{-(S_{A_j}^i - a^i)}{b^i{}^2}\right) \sigma_{ab}^i} \quad (\text{Eq. S2})$$

77 Where Δ_S^i is absolute uncertainty in the corrected signal (S_A^i multiplied by σ_S^i), Δ_a^i and Δ_b^i are the
 78 absolute uncertainty in the intercept and slope, respectively, and σ_{ab}^i is their covariance.
 79 Injections of only internal standard (lacking any calibrant) are used as zeroes to constrain the
 80 intercept. Inclusion of an intercept term therefore amounts to background subtraction, which is
 81 observed in most cases to be within uncertainty of the origin, suggesting background subtraction
 82 is minor and any error introduced is included in the error of the intercept term, Δ_a^i .

83 Error in mass can also be calculated empirically from the fit as the difference between measured
 84 and injected mass (NIST, 2014b)

$$85 \quad \Delta_{M_j}^i = M_{A_j}^i - (\text{mass injected}) \quad (\text{Eq. S3})$$

86 As signal approaches the intercept, the relative calibration error increases in importance due to
 87 the uncertainty in the intercept term, even when constrained by injections of “zeros”. This is
 88 demonstrated in Fig. S2, in which the uncertainty for calibration of pinic acid is calculated both
 89 formally from Eq. S2 (blue squares) and empirically from Eq. S3 (red circles) and normalized to
 90 the observed mass. The formal calculation is in good agreement with the empirical
 91 measurements.



92

93 Figure S2. Relative error in mass calibration of pinic acid during one operational period,
 94 calculated with the formal equation (blue) and as the residual of the linear fit for each point (red).

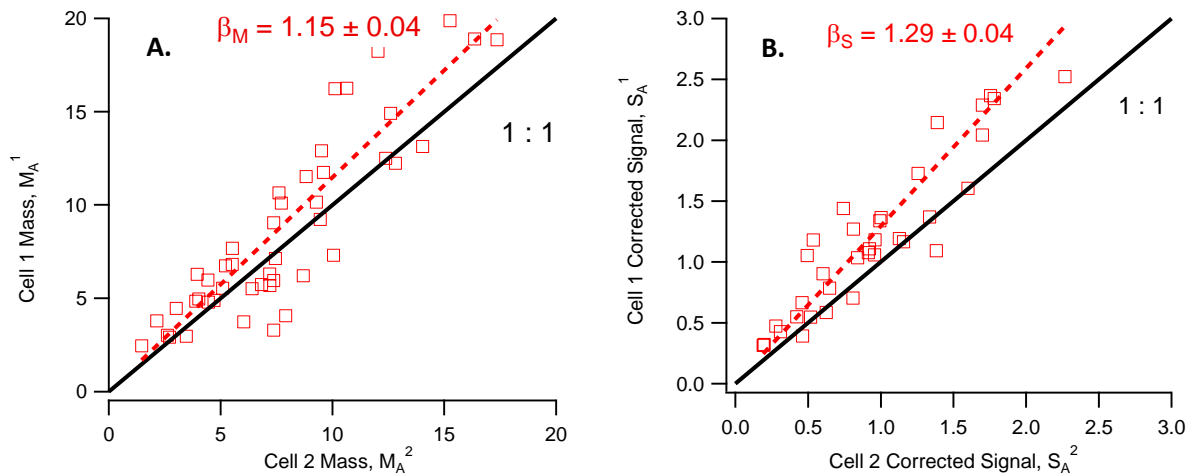
95

96 While Δ_M^i is point-specific, uncertainty in the intercept, Δ_a^i , is negligible for large samples so
 97 uncertainty for most points is dominated by error in the corrected signal and the slope, which are
 98 a constant fraction independent of measured mass. However, uncertainty can be very large at
 99 measured masses near the lower limit of the calibration range (Fig. S2). The detection limit for
 100 this compound (3 times the background chromatographic signal) is approximately 0.5 ng on
 101 column, in good agreement with Fig. S2 as uncertainty in the measurement approaches 100%
 102 near the detection limit. For compounds with concentrations typically higher than the detection
 103 limit, relative mass uncertainty, σ_M^i , can be considered to be 15% (assuming $\sigma_S^i = 10\%$), though
 104 it should be explicitly calculated for each compound. For cases in which most points fall well
 105 above detection limit, an average estimate of error for each compound is sufficient, though it is
 106 in all cases more desirable to report absolute uncertainty for each measurement when possible.

107 The uncertainty introduced by the intercept term is expected to be more important in denuded
 108 samples, where signals are typically lower, though including an adequate zero or blank
 109 measurement can help reduce this source of uncertainty. Consequently, it can reasonably be
 110 expected that M_A^{den} typically has a higher uncertainty than M_A^{byp} . The degree to which this is the
 111 case depends on uncertainty in the intercept term and the size of denuded signals relative to
 112 bypass signals, but suggests error will typically be lower in bypass samples.

113 **S3.2. Normalizing between cells**

114 In an ideal world, the parallel sampling cells are exactly the same, but this is not the case due to
115 small but consistent differences in derivatization efficiency and/or transfer losses not accounted
116 for by the calibration, so there is a need to correct for these differences. Generating continuous
117 timelines of mass concentrations or to calculate fraction in the particle relies on this correction
118 because during typical operation a sample is denuded on one cell and bypass on the other, then
119 the cells are switched to avoid bias. Variations on this sampling scheme can be employed, but in
120 all schemes there is a fundamental need to intercompare cells. To correct for systematic
121 differences between the cells, bypass samples are periodically collected simultaneously in both
122 cells, providing a direct comparison using real air samples. This comparison is shown in Fig. S3
123 using both fully calibrated masses (Fig. S3a) and uncalibrated signals (Fig. S3b). Note that
124 calibrating the signal reduces the difference between the cells, but also marginally increases the
125 relative uncertainty in the slope.



126
127 Figure S3. “Bypass-bypass” comparison of pinic between two cells, Cell 1 and Cell 2, in (a)
128 mass terms, M_A^1 and M_A^2 and (b) signal terms, S_A^1 and S_A^2 .

129 The bypass-bypass comparison of identical samples on the two cells prior to normalization
130 provides an equalization factor, E_M^i , to adjust the cells to their mean value. This equalization can
131 be applied across an entire measurement period, or to subsets thereof. It has been observed that
132 there can be some temporal variability in cell-to-cell differences, so when possible, equalization
133 is performed in small subsets, comparing only the bypass-bypass points nearest in time to each

134 point. This is unlikely to affect average calibrated values, but is expected to yield more accurate
 135 temporal and diurnal variability.

136 The equalization factor is calculated from the best-fit slope, β , (Fig. S3) which is forced through
 137 zero because sample cannot exist on one cell and not the other, so an intercept has no physical
 138 meaning. In most cases the intercept is within uncertainty of the fit so forcing through zero
 139 simplifies calculations with no detriment to the fit. The equalization factor is therefore:

$$140 \quad E_M^2 = 0.5(\beta + 1) \quad \text{and} \quad E_M^1 = 0.5\left(\frac{1}{\beta} + 1\right) \quad (\text{Eq. S4})$$

$$141 \quad \text{and, in relative terms, } \sigma_{E_M} = \sigma_{\beta_M} \text{ (in the shown example, approximately 4\%)} \quad (\text{Eq. S5})$$

142 To equalize the cells, the original mass calculated is multiplied by this factor:

$$143 \quad \text{Adjusted mass, } M_A^{i*} = E_M^i \times M_A^i \quad (\text{Eq. S6})$$

$$144 \quad \text{with error: } \sigma_{M_p}^{i*} = \sqrt{(\sigma_M^i)^2 + (\sigma_{E_M})^2} \quad (\text{Eq. S7})$$

145 This error accounts only for uncertainty in precision, designated with subscript p , which
 146 incorporates uncertainty in the equalization factor, σ_{E_M} , but does not account for systematic
 147 errors or instrument biases. The equalization factor is itself a systematic error in accuracy, while
 148 other additional instrument uncertainties, σ_I , may also contribute to accuracy error, to yield:

$$149 \quad \text{total error in mass measurement, } \sigma_M^{i*} = \sqrt{(\sigma_{M_p}^{i*})^2 + (\sigma_I)^2} \quad (\text{Eq. S8})$$

150 Because equalization modifies the absolute calibrated mass in each cell, systematic biases must
 151 be as great as or greater than the magnitude of the equalization factor. Additional known sources
 152 of error, i.e. uncertainty in sample volume, liquid injection, etc., may also cause systematic
 153 uncertainties and instrument errors. However, because cells are largely independent – i.e.
 154 separate sample volume control and liquid injection volumes – many potential significant
 155 sources of instrument error would negatively impact E_M . For example, if uncertainty in sample
 156 flow were 10%, it is unlikely the bypass-bypass comparison for any compounds would ever be in
 157 good agreement. Therefore, E_M incorporates in large part most other large uncertainties so is
 158 expected to be dominate instrument error:

$$159 \quad \text{total instrument error, } \sigma_I = |E_M - 1| + \sigma_1 + \sigma_2 + \dots \approx |E_M - 1| \quad (\text{Eq. S9})$$

160 Final precision uncertainty for the example compound (pinic acid) is therefore approximately
 161 15% (Eq. S7: $\sqrt{(15\%)^2 + (4\%)^2}$), with an additional bias error greater than 8% for a total error
 162 of approximately 20%. It should be noted that any compound for which an authentic standard
 163 error is unavailable has an additional bias error, which is in most cases difficult to constrain.

164

165 **S3.3. Uncertainty in Partitioning Fraction, F_P**

166 Fraction in the particle, F_P , is calculated by comparing a “bypass” sample in one cell to a
 167 simultaneously collected “denuded” sample in the other cell, which requires equalization
 168 between the cells. Though this can most intuitively be considered in mass terms, $F_{P,M}$, calculation
 169 of F_P relies solely on the ability to intercompare samples on different cells, not necessarily
 170 quantitative mass measurements. F_P can therefore also be considered in signal terms, using a
 171 signal-based equalization factor, which will be shown here to result in reduced uncertainty:

$$172 \quad F_{P,M} = \frac{M_A^{\text{den}}}{M_A^{\text{byp}}} \times \beta_M \quad \equiv \quad F_{P,S} = \frac{S_A^{\text{den}}}{S_A^{\text{byp}}} \times \beta_S \quad (\text{in the case where Cell 2 denuded}) \quad (\text{Eq. S10})$$

173 As a comparison between the cells, systematic biases in accuracy do not add uncertainty to this
 174 calculation. Instead, only uncertainty in precision and the equalization factor are relevant:

$$175 \quad \sigma_{F_{P,M/S}} = \sqrt{(\sigma_{M/S}^{\text{den}})^2 + (\sigma_{M/S}^{\text{byp}})^2 + (\sigma_{E_{M/S}})^2} \quad (\text{Eq. S11})$$

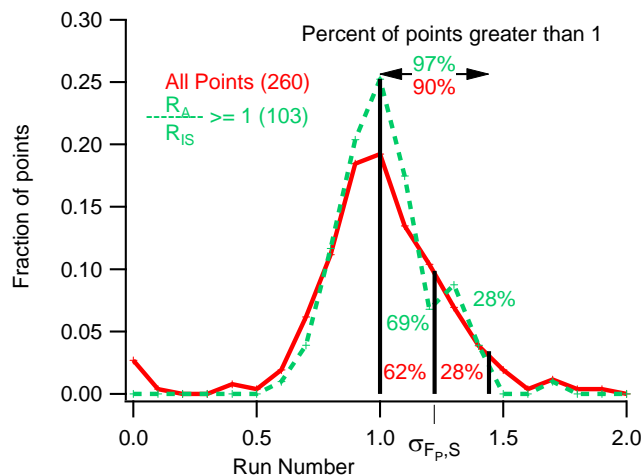
176 In signal terms, the bypass-bypass ratio, β , is expected to be higher than in mass terms, as is
 177 observed in Fig. S3. However, the magnitude of the equalization does adversely affect
 178 uncertainty in F_P because uncertainty in intercomparison between cells does not depend on the
 179 size of this equalization, only on the uncertainty in the ratio, which is similar or slightly lower in
 180 signal terms. Given that σ_M^i is a function of both signal uncertainty, σ_S^i , and calibration error,
 181 formulating Eq. S11 in signal terms using only σ_S^i necessarily yields lower uncertainty.

182 The formal calculation of error in Eq. S11 can be tested against an empirical error estimate by
 183 investigating scatter around the cell-to-cell equalization line in an ideal case. When the internal
 184 standard is very similar to the analyte, as in the example compound (pinic acid – $C_9H_{14}O_4$, using
 185 as an internal standard a deuterated adipic acid – $C_6H_6D_4O_4$), the scatter around the equalization

186 line, β , is a result of the uncertainties in corrected signals (σ_S^i) as well as any uncertainties in cell-
187 to-cell equalization and is therefore a good estimate of the error in F_P , similar to Eq. S3 (NIST,
188 2014b). The standard deviations of the residual from the equalization line for pinic acid in signal
189 and mass terms (Fig. S3) are 14% and 18% respectively, very similar to the calculated errors of
190 $\sigma_{F_P,S} \approx 15\%$ and $\sigma_{F_P,M} \approx 20\%$, so formal calculation of error is found to be reasonable.

191 If no internal standard is available that is similar to the analyte of interest, equalization using
192 bypass-bypass analyses may result in a bias when comparing bypass to denuded samples due to
193 compound differences in sensitivity to sample concentration. Instead, a formal estimation of
194 error from Eq. S11 is the best estimate because calculation of σ_S^i using the scenarios shown in
195 the main text does include error caused by differences between analyte and internal standard.
196 From the estimates in Table 1, an internal standard containing approximately the same number of
197 OH groups is sufficient to greatly reduce this error. However, a large suite of internal standards
198 is recommended and is typical in SV-TAG operation, allowing relatively unbiased measurement
199 of F_P for all compounds with a robust formally estimated error of 15-25%

200 It should be noted that particle fraction is calculated as the ratio of one cell to another, so a value
201 of greater than 1 is possible due to measurement uncertainties. Uncertainties are reported as
202 standard deviations, so greater than approximately 70% of points with a particle fraction greater
203 than 1 should be within uncertainty of 1.00, and compounds entirely in the particular phase are
204 expected to be measured as an approximately normal distribution around $F_P = 1$. An example of
205 such a compound is hydroxy glutaric acid (Fig. S4), which is calculated from Eq. S11 to have an
206 uncertainty, $\sigma_{F_P,S}$, of approximately 22% using deuterated hydroxy glutaric acid as an internal
207 standard. The distribution of points is centered on $F_P = 1.02 \pm 0.02$ (standard error) with a
208 distribution well-described by $\sigma_{F_P,S}$ (97% of points with $F_P > 1$ are within $2 \sigma_{F_P,S}$). Uncertainty
209 in the particle fraction is only a weak function of signal size as demonstrated by Fig. S4, in
210 which larger analyte signals (green line) have a slightly narrower distribution around $F_P = 1$ than
211 signals smaller than the internal standard (red line), which is approximately 4 times the level of
212 quantification. Therefore, due to errors in chromatographic integration and mass spectrometric
213 background signals, it is possible that the average estimation of error underpredicts uncertainty at
214 signals very close to the limit of detection.



215
 216 Figure S4. Histogram of fraction in particle, $F_{P,S}$, for hydroxy glutaric acid for all points (red),
 217 and for points greater than the internal standard (green). $\sigma_{F_{P,M/S}} = 22\%$ from Eq. S11.

218
 219 While the formal error estimate of partitioning relies on the precision of the instrument and the
 220 ability to compare the cells, systematic biases can exist that must be explored. Both penetration
 221 of gases through the denuder and loss of gases to the inlet, for instance, will bias the instrument
 222 toward a higher F_P . Using various forms of zeroes, no evidence is found in SOAS data for a non-
 223 negligible influence of either of these potential biases. However, such biases need to be
 224 considered and generally added into F_P error if appropriate.

225
 226 **References**

227 Kovats, E: Gas-chromatographische Charakterisierung organischer Verbindungen. Teil 1:
 228 Retentionsindices aliphatischer Halogenide, Alkohole, Aldehyde und Ketone, Helv. Chim. Acta,
 229 41(7), 1915-1932, doi:10.1002/hlca.19580410703, 1958

230 NIST/SEMATECH e-Handbook of Statistical Methods: Section 2.3.6.7.3. Comparison of check
 231 standard analysis and propagation of error. Available online at
 232 <http://www.itl.nist.gov/div898/handbook/mpc/section3/mpc3673.htm>, Accessed June 12, 2014a.

233 NIST/SEMATECH e-Handbook of Statistical Methods: Section 2.3.6.7.2. Uncertainty for linear
 234 calibration using check standards. Available online at
 235 <http://www.itl.nist.gov/div898/handbook/mpc/section3/mpc3672.htm>, Accessed June 12, 2014b.